MICROPOLAR FLOW PAST A STRETCHING SHEET

by

Kishore Kumar Sankara

Layne T. Watson

CS84006-R

MICROPOLAR FLOW PAST A STRETCHING SHEET

KISHORE KUMAR SANKARA

Department of Mathematics
Indian Institute of Technology
Madras - 600 036, INDIA

LAYNE T. WATSON

Department of Computer Science
Virginia Polytechnic Institute and State University
Blacksburg, VA 24061
U.S.A.

ABSTRACT

This paper studies the flow of an incompressible, constant density micropolar fluid past a stretching sheet. The governing boundary layer equations of the flow are solved numerically using a globally convergent homotopy method in conjunction with a least change secant update quasi-Newton algorithm. The flow pattern depends on three non-dimensional parameters. Some interesting results are illustrated graphically and discussed.

1. INTRODUCTION

Eringen [1], [2] introduced the concept of micropolar fluids to provide a mathematical model for the behaviour of fluids which exhibit certain microscopic effects arising from the local structure and micromotions of the fluid elements, such as polymeric fluids, liquid crystals and animal blood. Peddieson and McNitt [3] derived the boundary layer equations for a micropolar fluid and applied these to the problems of steady stagnation point flow, steady flow past a semi-infinite flat plate, and impulsively started flow past a flat plate. They obtained numerical results for the first two problems. Willson [4] studied the micropolar boundary layer flow near a stagnation point using the Karman-Pohlhausen technique. The boundary layer flow of a micropolar fluid over a semi-infinite flat plate was studied by Ahmadi [5]. Using a Runge-Kutta shooting method with Newton iteration Kummerer [6] studied the self similar laminar boundary layers in a micropolar fluid. Guram and Smith [7] investigated the stagnation flows of micropolar fluids with strong and weak interactions. They obtained numerical results using a fourth order Runge-Kutta method. Recently Gorla [8] obtained numerical results by a Runge-Kutta method for the micropolar boundary layer flow at a stagnation point on a moving wall.

In this paper we investigate the steady micropolar flow past a stretching sheet. We obtain the numerical solution of

the problem using a globally convergent homotopy method in conjunction with a quasi-Newton method.

2. GOVERNING EQUATIONS

The basic equations of motion and continuity for steady two dimensional flow of micropolar fluids in rectangular Cartesian coordinates xyz with the velocity vector $U = [u(x,y), v(x,y), 0]$ and the microrotation vector $\bar{\sigma} = [0, 0, \sigma(x,y)]$ are

$$\rho\left(u\frac{\partial u}{\partial x} + v\frac{\partial u}{\partial y}\right) = -\frac{\partial p}{\partial x} + (\mu + k)\left(\frac{\partial^2 u}{\partial x^2} + \frac{\partial^2 u}{\partial y^2}\right) + k\frac{\partial \sigma}{\partial y} \qquad \ldots(1)$$

$$\rho\left(u\frac{\partial v}{\partial x} + v\frac{\partial v}{\partial y}\right) = -\frac{\partial p}{\partial y} + (\mu+k)\left(\frac{\partial^2 v}{\partial x} + \frac{\partial^2 v}{\partial y^2}\right) - k\frac{\partial \sigma}{\partial x} \qquad \ldots(2)$$

$$\rho J\left(u\frac{\partial \sigma}{\partial x} + \frac{\partial \sigma}{\partial y}\right) = \gamma\left(\frac{\partial^2 \sigma}{\partial x^2} + \frac{\partial^2 \sigma}{\partial y^2}\right) - 2k\sigma + k\left(\frac{\partial v}{\partial x} - \frac{\partial u}{\partial y}\right) \qquad \ldots(3)$$

$$\frac{\partial u}{\partial x} + \frac{\partial v}{\partial y} = 0 \qquad \ldots(4)$$

where ρ, μ, p are the density, viscosity, and pressure respectively. Further γ is the microrotational coupling coefficient, k is the microrotational diffusivity, and J the square of a length typical of the microstructure. Eringen [2] showed through thermodynamic arguments that γ, k, and μ are all non-negative. Equations (1) - (3) reduce to the Navier-stokes equations for steady two dimensional flow of incompressible Newtonian fluids when $\gamma = k = J = 0$. The velocity and microrotation are uncoupled when $k = 0$ and the macroscopic motion is unaffected by the microrotations.

We consider the flow past a wall coinciding with the plane $y = 0$, and the flow is confined to $y > 0$. Keeping the origin fixed, the wall is stretched by introducing two equal and opposite

forces along the x - axis [see Fig. 1]. With the usual boundary layer assumptions equations (1) - (4) reduce to the following form:

$$u \frac{\partial u}{\partial x} + v \frac{\partial u}{\partial y} = \nu \frac{\partial^2 u}{\partial y^2} + K \frac{\partial \sigma}{\partial y} \quad , \qquad \ldots\ldots(5)$$

$$\tilde{J}\left(u \frac{\partial \sigma}{\partial x} + v \frac{\partial \sigma}{\partial y}\right) = G \frac{\partial^2 \sigma}{\partial y^2} - 2\sigma - \frac{\partial u}{\partial y} \quad , \qquad \ldots\ldots(6)$$

$$\frac{\partial u}{\partial x} + \frac{\partial v}{\partial y} = 0 \quad , \qquad \ldots\ldots(7)$$

with $\nu = \frac{\mu + k}{\rho}$, $K = \frac{k}{\rho}$, $G = \frac{\gamma}{k}$, $\tilde{J} = \frac{J\rho}{k}$.

The boundary conditions are

$$u = Cx \ , v = 0, \ \sigma = 0 \quad \text{at } y = 0 \quad , \qquad \ldots\ldots(8)$$

$$u \longrightarrow 0 \ , \ \sigma \longrightarrow 0 \quad \text{as } y \longrightarrow \infty \quad , \qquad \ldots\ldots(9)$$

where $C > 0$.

Using the transformations

$$u = Cx \, f_1'(\eta) \quad , \qquad \ldots\ldots(10)$$

$$v = -(\nu C)^{1/2} f_1(\eta) \quad , \qquad \ldots\ldots(11)$$

$$\sigma = (C^3/\nu)^{1/2} x f_2(\eta) \quad , \qquad \ldots\ldots(12)$$

$$\eta = (C/\nu)^{1/2} y \quad , \qquad \ldots\ldots(13)$$

equations (5) - (7) reduce to the following form:

$$f_1''' = - f_1 f_1'' + (f_1')^2 - C_1 f_2' \quad , \qquad \ldots\ldots(14)$$

$$f_2'' = \frac{1}{C_2} [f_1'' + 2f_2 - C_3(f_1 f_2' - f_1' f_2)/C_1] \quad , \qquad \ldots\ldots(15)$$

with the non-dimensional parameters

$$C_1 = \frac{K}{\nu} \; ; \; C_2 = \frac{GC}{\nu} \; , \; C_3 = \frac{JC}{\nu} \qquad \ldots.(16)$$

The boundary conditions corresponding to (14) and (15) are

$$f_1 = 0, \; f_1' = 1 \; , \; f_2 = 0 \text{ for } \eta = 0 \; , \qquad \ldots.(17)$$

$$f_1' \longrightarrow 0, \; f_2 \longrightarrow 0 \text{ as } \eta \longrightarrow \infty \; . \qquad \ldots.(18)$$

3. METHOD OF SOLUTION

Define $\underline{V} = \begin{pmatrix} f_1''(0) \\ f_2'(0) \end{pmatrix}$ ....(19)

and let $f_1(\eta; \underline{V})$, $f_2(\eta ; \underline{V})$ denote the solution of the initial value problem given by (14), (15) with initial conditions (17) and (19). Now note that the original two point boundary value problem (14) - (18) is equivalent (numerically) to solving the non-linear system of equations

$$F(\underline{V}) = \begin{pmatrix} f_1'(\tau ; \underline{V}) \\ f_2(\tau ; \underline{V}) \end{pmatrix} = 0 \qquad \ldots.(20)$$

where τ is chosen large enough so that $|f_1(\eta) - f_1(\tau)| < \epsilon$ and $|f_2(\eta)| < \epsilon$ for $\tau \leq \eta < \infty$ and a given $\epsilon > 0$.

Algorithms for solving the non-linear system (20) typically require partial derivatives such as $\frac{\partial f_2}{\partial \underline{V}_k}$. These dervatives are calculated as follows:

Let $Y = \Big(f_1(\eta)$, $f_1'(\eta)$, $f_1''(\eta)$, $f_2(\eta)$, $f_2'(\eta)$,

$$\frac{\partial f_1(\eta)}{\partial \underline{V}_k}, \frac{\partial f_1'(\eta)}{\partial \underline{V}_k}, \frac{\partial f_1''(\eta)}{\partial \underline{V}_k}, \frac{\partial f_2(\eta)}{\partial \underline{V}_k}, \frac{\partial f_2'(\eta)}{\partial \underline{V}_k}\Big) .$$

Then $f_1(\eta ; \underline{V})$, $f_2(\eta ; \underline{V})$ and their partial derivatives with respect to η and $\underline{V}_k$ $(k = 1,2)$ can be calculated from the first order system

$$Y_1' = Y_2$$

$$Y_2' = Y_3$$

$$Y_3' = - Y_1 Y_3 + Y_3^2 - C_1 Y_5$$

$$Y_4' = Y_5$$

$$Y_5' = \left[Y_3 + 2 Y_4 - \frac{C_3}{C_1} (Y_1 Y_5 - Y_2 Y_4) \right] / C_2$$

$$Y_6' = Y_7$$

$$Y_7' = Y_5$$

$$Y_8' = - Y_1 Y_8 - Y_6 Y_3 + 2 Y_2 Y_7 - C_1 Y_{10}$$

$$Y_9' = Y_{10}$$

$$Y_{10}' = \left[Y_8 + 2 Y_9 - \frac{C_1}{C_3} (Y_1 Y_{10} + Y_6 Y_5 - Y_2 Y_9 - Y_7 Y_4) \right] / C_2$$

$$Y(0) = (0, 1, \underline{V}_1, 0, \underline{V}_2, 0, 0, \delta_{1k}, 0, \delta_{2k})$$

By solving this system twice, for k = 1 and k = 2, the Jacobian matrix $DF(\underline{V})$ of $F(\underline{V})$ can be calculated.

The nonlinear system of equations (20) is solved by a globally convergent homotopy method. Such methods are necessary for highly non-linear problems like equations (20), since locally convergent methods like Newton's method diverge unless

the starting point is very close to the solution and quasi-Newton methods frequently converge to spurious solutions. Considerable computational experience with non-linear systems of equations arising from fluid mechanics problems (Watson et.al.[9], Wang and Watson, [10,11], Watson [12]) indicates that such globally conververgent methods are indeed necessary, unless, of course, one is willing to solve a large number of non-linear systems, varying the parameters slowly. A brief description of a globally convergent homotopy method is given here; see Watson [13], Watson and Fenner [14], or Watson [15] for the theory, algorthmic details, and other applications. Let E^2 denote two dimensional Euclidean space, $a \in E^2$, and define the homotopy map $\rho_a : [0,1) \times E^2 \longrightarrow E^2$ by

$$\rho_a(\lambda, \underline{V}) = \lambda F(\underline{V}) + (1-\lambda)(\underline{V} - a) \qquad \ldots(21)$$

The supporting theory says that under fairly general assumptions, for almost all a the Jacobian matrix $D\rho_a(\lambda, \underline{V})$ of the map $\rho_a(\lambda, \underline{V})$ has full rank at zeros of ρ_a, and there is a smooth zero curve γ_1 of ρ_a emanating from $(0,a)$ and reaching a solution $\bar{\underline{V}}$ of $F(\underline{V}) = 0$ at $\lambda = 1$. Conceptually the homotopy algorithm is simple ; just follow the zero curve γ_1 until it reaches the solution $\bar{\underline{V}}$. Note that λ is ''artificial'', and not a natural parameter of the problem. Parametrize γ_1 by arc length s, so $\lambda = \lambda(s)$, $\underline{V} = \underline{V}(s)$ along γ_1. Then

$$\frac{d}{ds}\rho_a(\lambda(s), \underline{V}(s)) = D\rho_a\left(\lambda(s), \underline{V}(s)\right)\begin{pmatrix} d\lambda/ds \\ d\underline{V}/ds \end{pmatrix} = 0 \qquad \ldots(22)$$

identically in s. Now γ_1 is precisely the trajectory of the initial value problem (22) with initial conditions.

$$\lambda(0) = 0 \ , \ \underline{V}(0) = a \ . \qquad \ldots\ldots(23)$$

Hence tracking γ_1 amounts to solving (22) and (23) until the point $(1,\underline{\bar{V}})$ is reached. Because the Jacobian matrix $D\rho_a(\lambda,\underline{V})$ has full rank , and s rather than λ is the independent variable, turning points of γ_1 pose no special difficulties whatsoever. The power of this homotopy algorithm, compared to standard continuation, derives from the ability of λ to both increase and decrease along γ_1. The numerical solution of the initial value problem (22,23) is not straightforward, since the derivative $(d\lambda/ds, d\underline{V}/ds)$ is only given implicitly by (22). Details of the numerical algorithm are in Watson [5].

Quasi-Newton methods, such as those implemented in Argonne National Laboratory's MINPACK [16] subroutine package, are robust and much more efficient than a globally convergent homotopy such as the one used here. However, quasi-Newton methods frequently fail by converging to spurious solutions of $F(\underline{V}) = 0$ (critical points of $F(\underline{V})^tF(\underline{V})$ which do not satisfy $F(\underline{V}) = 0$). Hence the overall strategy is to try a cheap quasi-Newton algorithm first, and if that fails, then resort to the expensive but guaranteed homotopy algorithm. Here the quasi-Newton algorithm was generally successful for small parameter values or small τ, and failed for large parameter values and large τ without a close initial estimate.

4. CONCLUSIONS

The values of the parameters C_1,C_2, and C_3 chosen in the present investigation are based on the inequalities $\mu > 0$, $K \geq 0$, $\gamma \geq 0$, $J > 0$ for micropolar fluids (see Eringen [2]). C_1 may take on values in the range $0 \leq C_1 < 1$. While $C_1 = 0$ corresponds to the case of uncoupled equations, $C_1 \longrightarrow 1$ corresponds to the limiting case of infinite coupling parameter K. The values of C_2 and C_3 are always non-negative. While only very small values of C_3 are of interest as J is the square of length typical of the microstructure, C_2 may vary over a larger range.

Figure 2(a) and 2(b) represent the velocity profiles in the transverse direction. It can be observed from these figures that the velocity towards the sheet decreases as C_1 increases and is insensitive to changes in C_3. Figures 3(a) and 3(b) represent the velocity profiles f_1' along the sheet. f_1' decreases as C_1 increases but little change is found in the flow pattern as C_3 changes.

Microrotation profiles are shown in Figures 4(a),(b),(c). From these figures it can be observed that microrotation velocity reaches a maximum at a finite distance from the wall. For given values of C_1 and C_3, increasing values of C_2 result in a decrease of the microrotation velocity with an increase in the boundary layer thickness as the maximum moves away from the wall. This is seen from Figure 4(a). From Figure 4(b) it

can be observed that for given values of C_2 and C_3, increasing values of C_1 result in increasing the microrotation velocity with an increase in the boundary layer thickness as the maximum moves away from the wall. The dotted line in Figure 4(b) corresponds to the limiting case of infinite coupling ($C_1 = 1$), and the sensitivity of the microrotation velocity for small C_1 is also shown. Figure 4(c) shows yet another kind of behavior for given values of C_1 and C_2 and increasing values of C_3. The microrotation velocity and boundary layer thickness decrease as the maximum moves toward the wall.

Figures 5(a,b) show the variation of wall couple stress $f_2'(0)$ as a function of C_3 for various values of C_1 and C_2. The wall couple stress decreases as C_3 or C_2 increases and increases with C_1 for given C_2 and C_3. This observation can also be made from Table 1, where the values of shear stress and couple stress at the wall are given. For given values of C_1 and C_2 an increase in C_3 causes only a slight increase in wall shear stress $-f_1''(0)$. Similarly for given values of C_1 and C_3 an increase in C_2 causes only a slight increase in wall shear stress. But for given values of C_2 and C_3 an increase in C_1 causes significant decrease in wall shear stress.

REFERENCES

[1] A. C. Eringen, Int. J. Engng. Sci., 2, 205 (1964).

[2] A. C. Eringen, J. Math. Mech., 16, 1 (1966).

[3] J. R. John Peddieson and R. P. McNitt, Rec. Adv. Eng. Sci., 5, 405 (1970).

[4] A. J. Willson, Proc. Camb. Phil. Soc., 67, 469 (1970).

[5] G. Ahmadi, Int. J. Engng. Sci., 16, 639 (1976).

[6] H. Kummerer, Rheol. Acta, 16, 261 (1977).

[7] G. S. Guram and A. C. Smith, Comp. Maths. with Appls. 6, 213 (1980).

[8] R. S. R. Gorla, Int. J. Engng. Sci., 21, 25 (1983).

[9] L. T. Watson, T. Y. Li and C. Y. Wang, J. Appl. Mech., 45, 435 (1978).

[10] C. Y. Wang and L. T. Watson, Appl. Sci. Res., 35, 195 (1979).

[11] C. Y. Wang and L. T. Watson, ZAMP, 30, 773 (1979).

[12] L. T. Watson, J. Comput. Appl. Math., 7, 21 (1981).

[13] L. T. Watson, Appl. Math. Comput., 5, 297 (1979).

[14] L. T. Watson and D. Fenner, ACM Trans. Math. Software, 6, 252 (1980).

[15] L. T. Watson, Appl. Math. Comput., 9, 111 (1981).

[16] J. J. More, B. S. Garbow, and K. E. Hillstrom, User Guide for MINPACK-1, ANL-80-74, Argonne National Laboratory (1980).

FIGURE CAPTIONS

Figure 1: Physical model and coordinate system.

Figure 2: Transverse velocity distribution for f_1.

a) $C_2 = 4.5$, $C_3 = .01$, $C_1 = .001, .1, .5, 1.0$ (top to bottom)

b) $C_2 = 4.5$, $C_3 = 0.0$, $C_1 = .001, .1, .5, 1.0$ (top to bottom)

Figure 3: Velocity distribution for f_1'.

a) $C_2 = 4.5$, $C_3 = 0.0$, $C_1 = .001, .1, .5, 1.0$ (top to bottom)

b) $C_2 = 4.5$, $C_3 = .01$, $C_1 = .001, .1, .5, 1.0$ (top to bottom)

Figure 4: Microrotation velocity f_2.

a) $C_1 = .01$, $C_3 = 0$, $C_2 = 1.0, 1.5, 3.5, 6.0, 10.0$ (top to bottom)

b) $C_2 = 4.5$, $C_3 = .01$, $C_1 = .001, .1, .5, 1.0$ (bottom to top)

C) $C_1 = .01$, $C_2 = 1.5$, $C_3 = 0.0, .02, .05$ (top to bottom)

Figure 5: Wall couple stress $f_2'(0)$ as a function of C_3.

a) $C_2 = 1.5$, $C_1 = 1.0, .5, .1, .01$ (top to bottom)

b) $C_2 = 3.5$, $C_1 = 1.0, .5, .1, .01$ (top to bottom)

Table 1: Wall shear stress and wall couple stress.

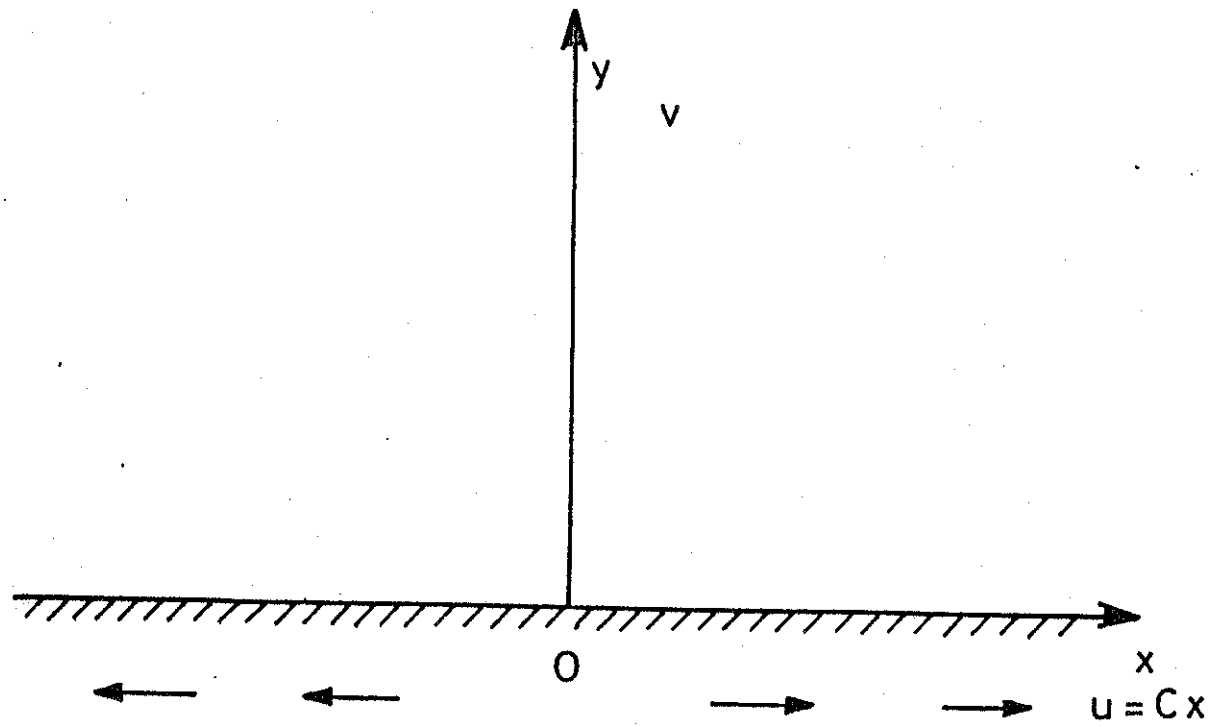

FIGURE.1.

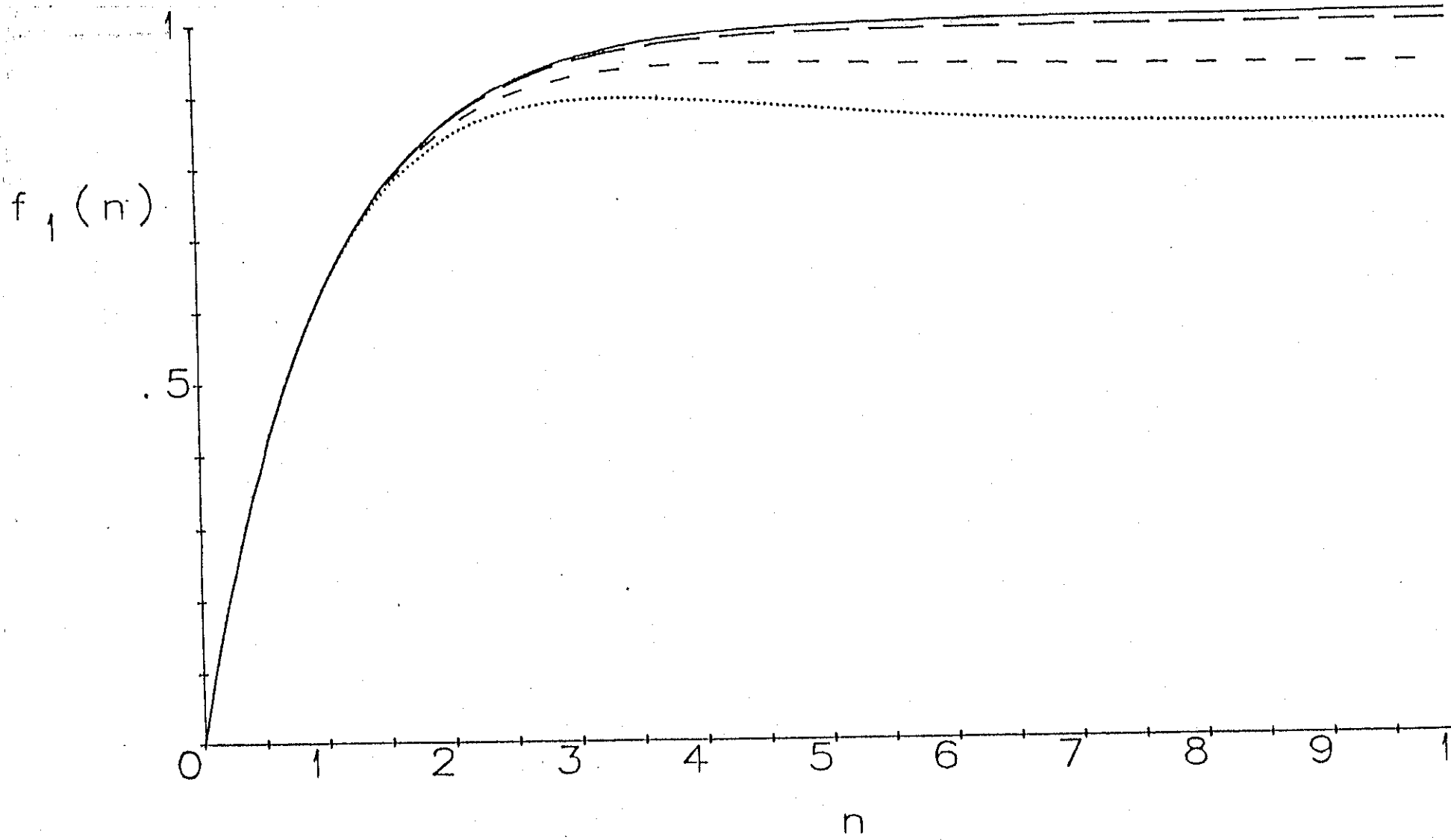

Fig. 2a

$c_2 = 4.5,\ c_3 = .01,\ c_1 = .001, .1, .5, 1.0$

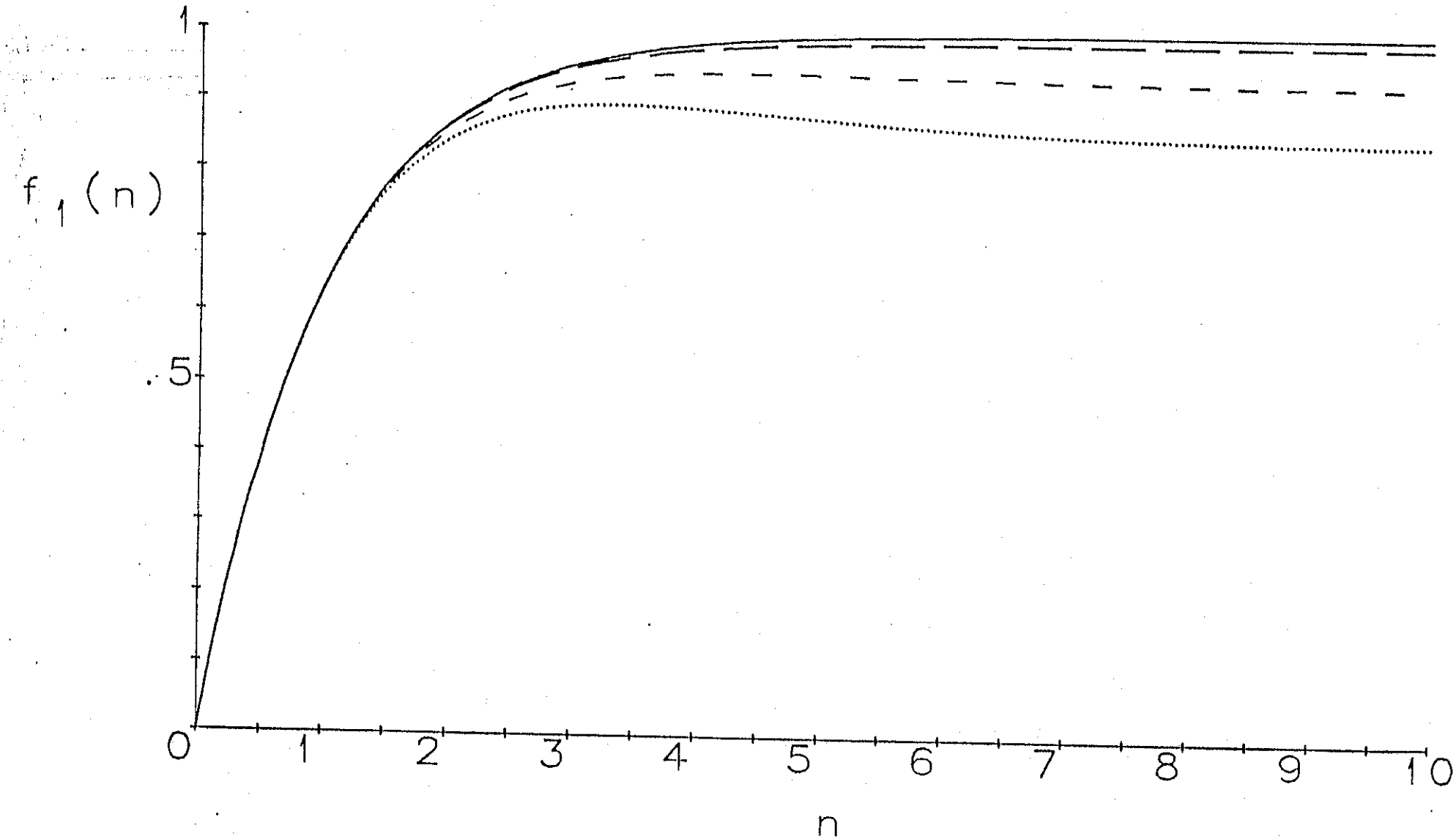

Fig. 2b $c_2 = 4.5,\ c_3 = 0,\ c_1 = .001,\ .1,\ .5,\ 1.0$

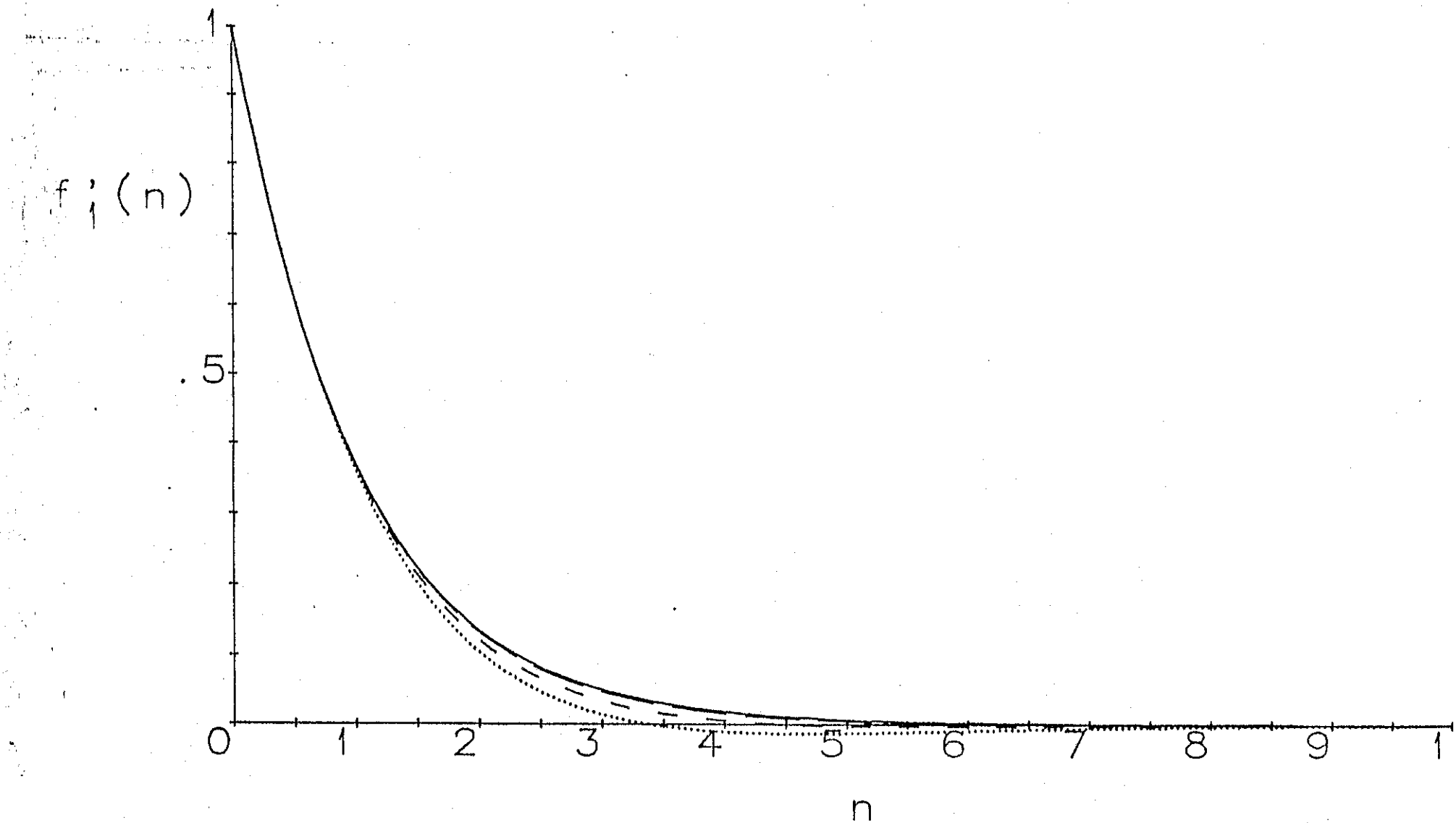

Fig. 3a

$c_2 = 4.5,\ c_3 = 0,\ c_1 = .001,\ .1,\ .5,\ 1.0$

Fig. 3b

$c_2 = 4.5,\ c_3 = .01,\ c_1 = .001,\ .1,\ .5,\ 1.0$

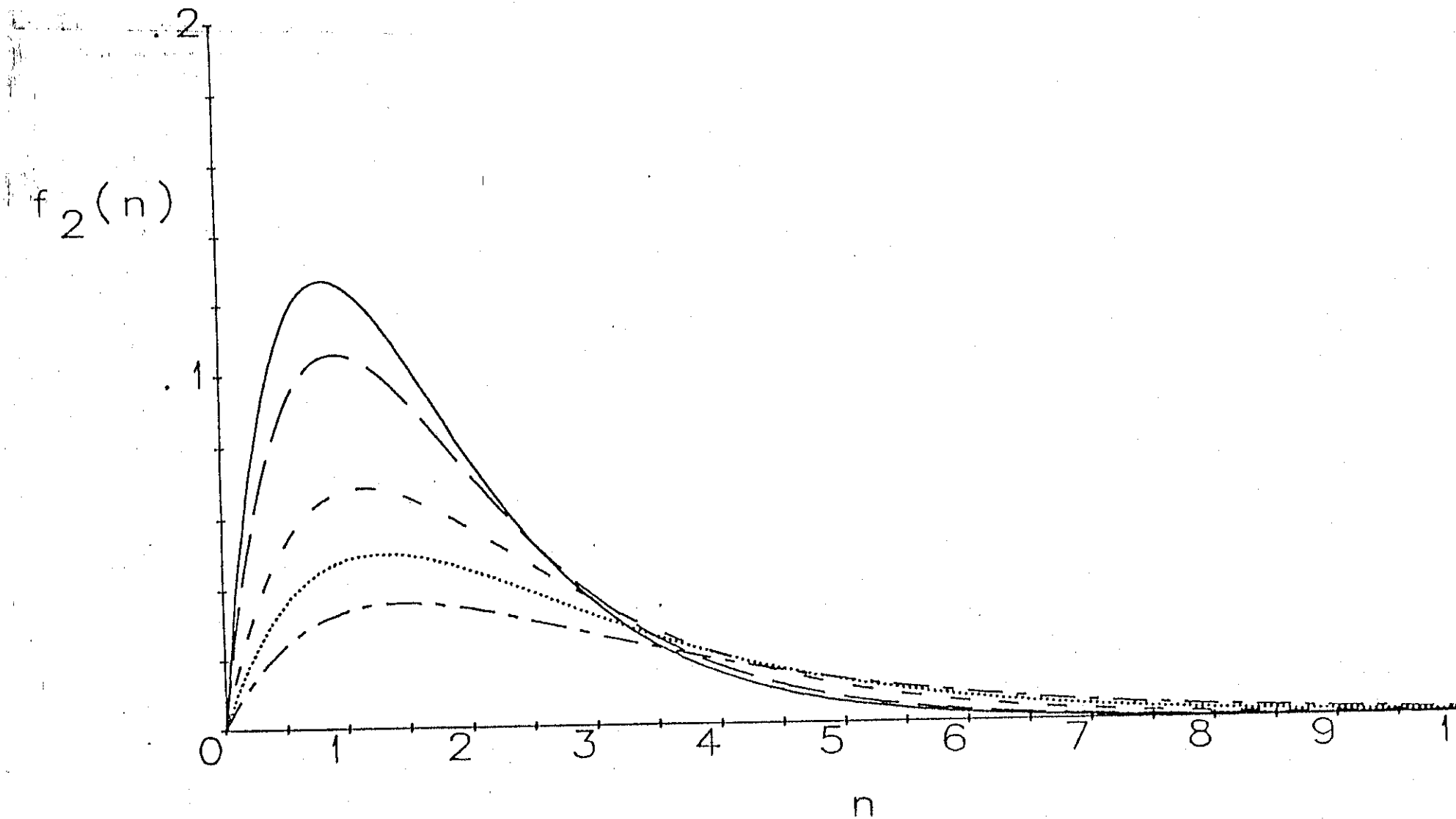

Fig. 4a

$c_1 = .01$, $c_3 = 0$, $c_2 = 1.0, 1.5, 3.5, 6.0, 10.0$

Fig. 4b

$C_x = 4.5,\ C_3 = .01,\ C_1 = .001, .1, .5, 1.0$

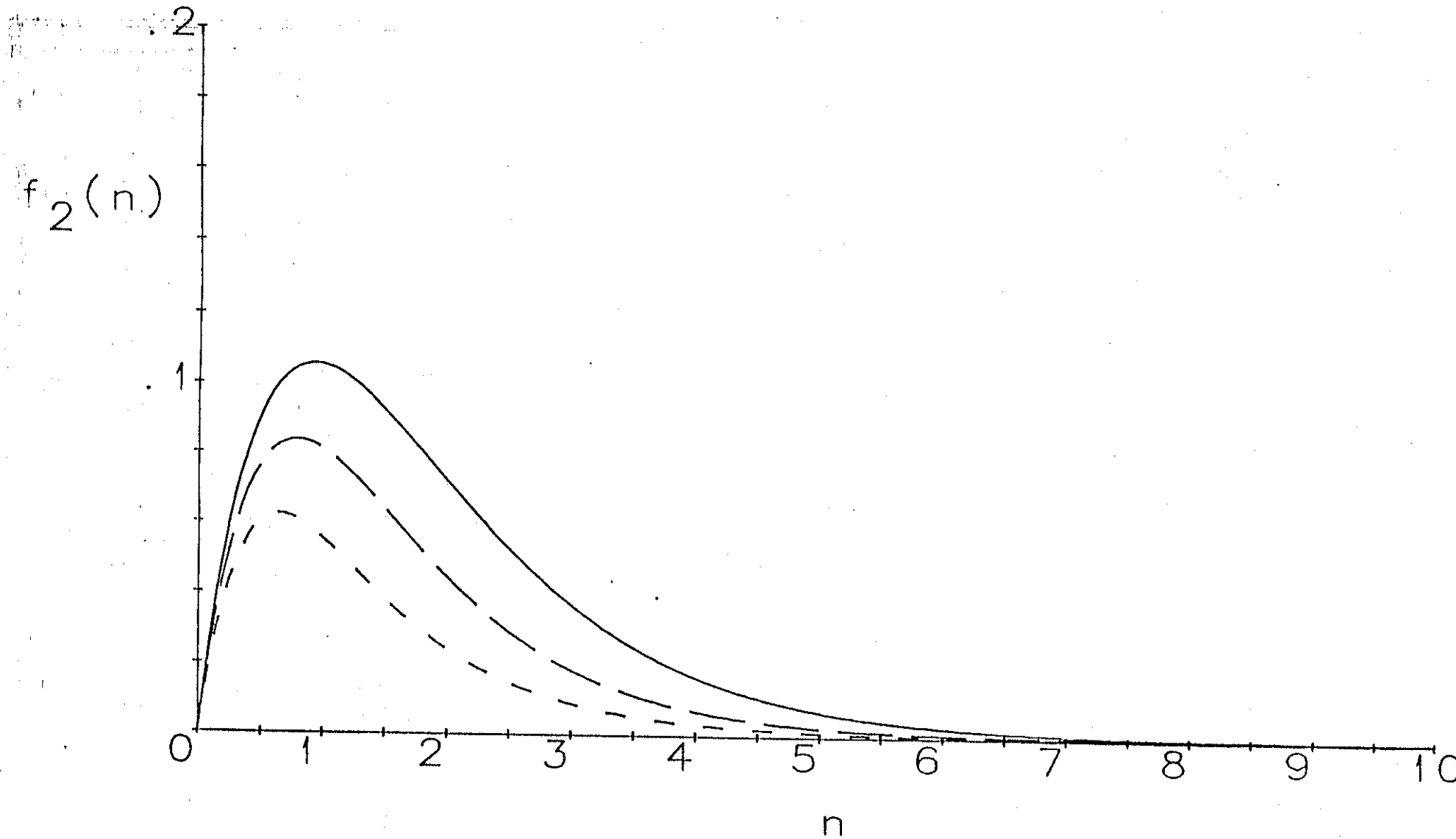

Fig. 4c

$c_1 = .01,\ c_2 = 1.5,\ c_3 = 0.0, .02, .05$

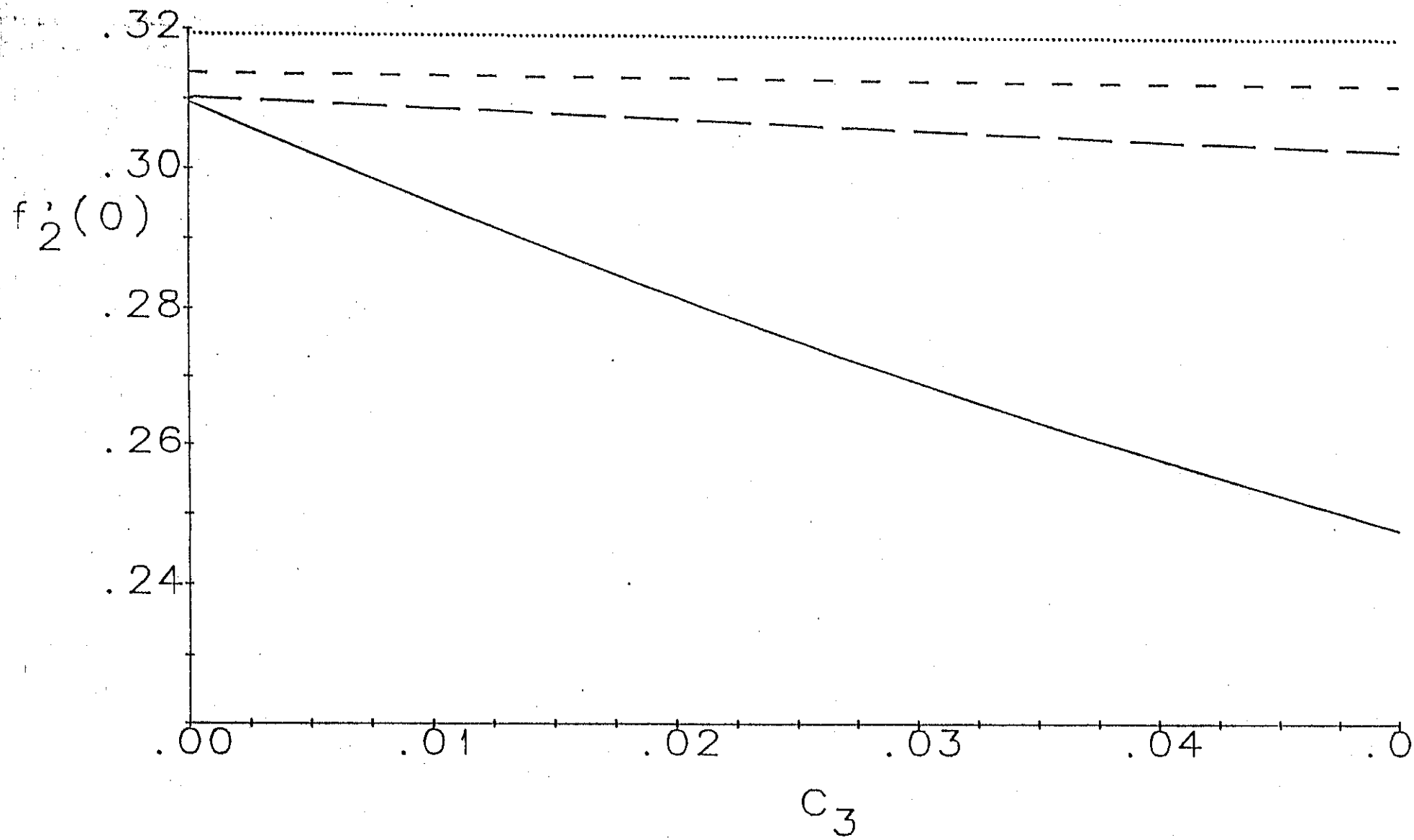

Fig. 5a

$c_1 = .01, .1, .5, 1.0$ $c_2 = 1.5$

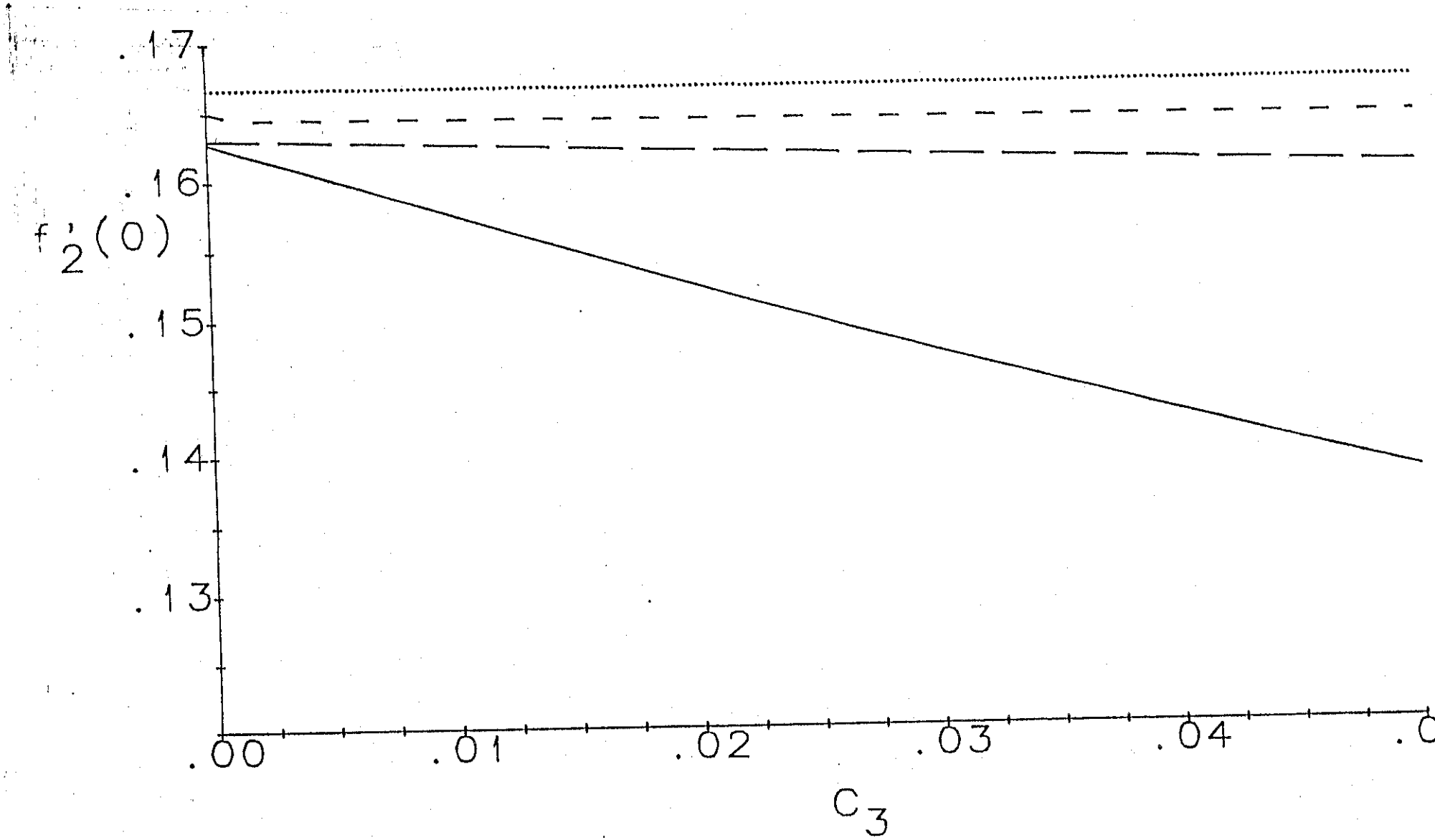

Fig. 5b

$c_1 = .01, .1, .5, 1.0$, $c_2 = 3.5$

	C1=.01, C3=0.0		C1=.01, C3=.05		C1=1.0, C3=0.0		C1=1.0, C3=.05	
C2	f1''(0)	f2'(0)	f1''(0)	f2'(0)	f1''(0)	f2'(0)	f1''(0)	f2'(0)
1.0	-.999345	.414323	-.999633	.322874	-.933203	.428800	-.933585	.427534
1.5	-.999464	.309477	-.999676	.247929	-.945854	.319311	-.946104	.318498
2.5	-.999594	.211192	-.999731	.175357	-.959516	.216944	-.959655	.216500
3.5	-.999668	.162746	-.999767	.138340	-.967086	.166667	-.967179	.166378
4.5	-.999717	.133357	-.999793	.115315	-.972019	.136257	-.972086	.136051
6.0	-.999765	.105679	-.999820	.093120	-.976942	.107699	-.976988	.107560
10.0	-.999836	.069107	-.999865	.062787	-.983957	.070127	-.983980	.070061

Table 1.

$